Front. Chem. Sci. Eng. 2021, 15(6): 1444–1461
https://doi.org/10.1007/s11705-021-2090-6

REVIEW ARTICLE

Hierarchically porous zeolites synthesized with carbon materials as templates

Huan Wang, Guo Du, Jiaqing Jia, Shaohua Chen, Zhipeng Su, Rui Chen, Tiehong Chen (✉)

Institute of New Catalytic Materials Science, School of Materials Science and Engineering, Key Laboratory of Advanced Energy Materials Chemistry (MOE), Nankai University, Tianjin 300350, China

Abstract Hierarchically porous zeolites are promising candidates in catalytic conversion of relatively bulky molecules, and their syntheses have attracted significant attention. From both industrial and scientific perspectives, different carbon materials have been widely employed as hard templates for the preparation of hierarchically porous zeolites during the past two decades. In this review, the progress in synthetic strategies using carbon materials as templates is comprehensively summarized. Depending on the affinity between the carbon templates and zeolite precursors, the substantial strategies for synthesizing hierarchical zeolites are introduced in direct templates and indirect templates. Direct templates methods, by which the carbon materials are directly mixed with precursors gel as hard templates, are first reviewed. Then, we discuss the indirect templates method (crystallization of carbon-silica composites), by which the carbon is produced by *in situ* pyrolysis of organic-inorganic precursors. In addition, the technique of encapsulating metal species into zeolites crystals with the assistance of carbon templates is also discussed. In the conclusion part, the factors affecting the synthesis of carbon-templated hierarchically porous zeolites are remarked. This review is expected to attract interest in the synthesis strategies of hierarchically porous zeolites, especially cost-effective and large-scale production methodologies, which are essential to the industrial application of hierarchical zeolites.

Keywords hierarchical zeolites, carbon materials, direct templates, indirect templates, carbon-silica composites

Received April 20, 2021; accepted July 5, 2021

E-mail: chenth@nankai.edu.cn

1 Introduction

With well-defined micropores, strong intrinsic acidity, and high (hydro)thermal stability, zeolites have been industrially used in the field of gas adsorption-separation, heterogeneous catalysis, and ion exchange [1]. However, the limited accessibility inherited from the subnanometer-scale micropore of zeolites strongly restricts the catalytic performance for conversion of bulky molecules. Great effort has been devoted to the fabrication of zeolites with hierarchical porosity to integrate shape selectivity of micropores and enhanced mass transfer of auxiliary porosity system. Furthermore, hierarchically porous zeolites possess the merits of modulating the product's selectivity, inhibiting rapid deactivation, and improving utilization of active sites located inside the channel.

Various innovative strategies for the preparation of hierarchically porous zeolites are mainly divided into post-synthesis (dealumination and desilication) [2–5], soft templating [6–16], hard templating [17–22] and other approaches [23–25]. Post-synthetic treatment suffers from the destruction of microporous architecture, low product yield, and limitation by framework composition. Soft templates, such as surfactant [6–8], amphiphilic organosilane [9–11], and supramolecular polymer [12–16], are generally expensive, which are unrealistic for large-scale industrialization. What's more, hard templating routes have been developed, and readily available carbon materials [17,18], SiO_2 [19,20], polymer [21], and $CaCO_3$ [22], etc. have been served as solid templates. Among the numerous hard templates, carbonaceous materials are mostly employed because of the controllable structure, tunable pore size, diverse morphologies, and easily modified surface. The reported carbon templates include carbon black nanoparticles [26], carbon nanotubes (CNTs) [17], carbon aerogel [27], graphite oxide (GO) [28], ordered mesoporous carbon (CMK-n) [29] and colloid-imprinted carbon [18], and so on. Recently, the

research on the crystallization of carbon-silica composites has received extensive attention. The tight connection between carbon and silica is beneficial for the well-penetration of carbon solid into the crystallized zeolite particles. For carbon-templated zeolites, the regularity and interconnectivity of macro/mesopores are strongly related to many factors, such as channel structure, morphology, the particle size of carbon, and the interaction between the templates and the zeolites precursors.

In this review, we focus on the synthesis of carbon-templated zeolites with pore hierarchy. First, the recent progress in the direct templates method is reviewed (Section 2). The additional carbon templates are directly immersed into zeolite precursor mixture, which consisted of microporous structure-directing agent, alkali source, Si source, and Al source. The adopted crystallization approaches mainly include hydrothermal synthesis (HTS, Section 2.1) and dry gel conversion (DGC, Section 2.2). Then, the achievements of the indirect templates method, which referred to the zeolitization of the carbon-silica composites, are elaborated (Section 3). The typical process involves infiltration of the composite with the structure-directing agent and then crystallization at high temperature. These composites are summarized in sections of CMK-n-silica composites (Section 3.1), carbon-coated silica composites (Section 3.2), and carbon-silica monolithic composites (Section 3.3). Finally, we discuss the functionalization of the zeolites by encapsulating metal species with carbon templates (Section 4).

With the substantial achievements and significant advantages of the hierarchical zeolites, there have been reviews focusing on the carbon templated zeolites. Here, we present recent progress in the direct-templates method according to different synthetic procedures, emphasizing the advantages and limitations of each approach. Furthermore, the indirect-templates process with benefits, such as highly efficient utilization of carbon, is particularly emphasized to inspire more attention in this field. Besides, we also mention the current challenges and future perspectives in carbon-templating methods for hierarchically porous zeolites.

2 Direct templates

The direct templates method refers to the strategy of constructing hierarchical zeolites using additional carbon materials as hard templates, which is generally applied to create porosity during crystallization. The added carbon templates are dispersed into the zeolite precursor gel/solution and then be encapsulated in the zeolite crystal particles. Due to the chemically inert characteristic and controllable size, various carbon materials, such as carbon nanoparticles, CNTs, biomass-derived carbon, GO, three-dimensionally macro/mesoporous carbon, and CMK-n carbon, are widely used as sacrificial templates. In general, these strategies can be subdivided into two main categories: HTS and DGC.

2.1 Hydrothermal synthesis

Among the synthetic strategies of zeolites, the HTS method exhibit inherent flexibility and versatility in the fabrication of zeolites with different architectures and compositions. In a typical procedure, the solid carbon templates are evenly mixed into the zeolite precursor, and the resulting mixture is subjected to one-pot hydrothermal treatment in a Teflonlined steel autoclave. The removal of carbon is accomplished by calcination under air, during which the occupied space is released, and the porosity is created in zeolites.

Carbon nanoparticles, such as commercial BP 2000, formed by incomplete combustion of petroleum residues, have been served as hard templates for hierarchically mesoporous zeolites by the HTS process [30,31]. The morphology of the used templates significantly affected the connectivity of the auxiliary porosity in the zeolites. Using carbon nanoparticles as secondary templates, hierarchical silicoalumophosphate (SAPO)-34 with isolated pores located inside the solid, was generated. Contrarily, with the addition of the CNTs, the produced SAPO-34 possessed intracrystalline pores accessible from the surface of the particle [32]. Then, various zeolites containing interconnected pores, such as ZSM-5 [33], SAPO-34 [34], Beta [35], silicalite-1 [36], were formed with the aid of CNTs, and the size of the mesopores usually matched with the diameter of the CNTs wrapped in the crystals. However, the high cost of CNTs inhibited their large-scale application. Due to the tailorable porosity, facile preparation, low cost, and obtainable in monolithic form, carbon aerogels were also investigated as potential templates for the generation of intracrystalline mesoporous zeolites [37,38]. The obtained monolithic zeolites with abundant and uniform pores were expected in the catalytic application, because of the greater accessibility to the active sites and the rigid mechanical strength. Since sustainable raw materials and cost-effectivity, biomass-derived carbon materials, such as sugar/protein-derived *N*-doped carbonaceous monolith [39], pyrolyzed wood [40] were considered. The possibility of extending the synthetic process to other biomass-derived materials and other zeolites framework structures is worth exploring. However, biomass material is the most abundant and renewable resource for the production of carbon templates, but the energy consumed in the pyrolysis process is still a limiting factor for industrial-scale preparation.

The critical issue of the HTS is the incompatibility of inert carbon in the precursor sol system. Due to the hydrophobic surface of ordinary carbon materials, the frail binding force between solid matrix and precursor solution would induce serious phase segregation. As predicted, GO with hydrophilic oxygen-containing groups could disperse

in gel very well, and some studies of GO templated zeolites were reported. The readily dispersed GO blocked the further growth of zeolite units, resulting in well-connected pores [28]. Some researchers even demonstrated the intergrowth of the silicalite-1 zeolite-GO composites. SEM observation indicated that silicalite-1 crystals grew on the surface of GO nanosheets. The affinity between GO templates and zeolite framework was the decisive factor in producing zeolite-GO composites [41]. The hydrophobic graphene was also used to synthesize zeolites, and the size and morphologies of the crystallized particles changed remarkably with the addition of graphene. Due to the hindering effect of the physical barriers on the growth of nanocrystals, the synthesized zeolites became significantly smaller as the amounts of employed graphene increased [42]. The particle-shaping role of the hydrophobic graphene is claimed, which is different from the pore-directing effect of hydrophilic GO in the synthetic system of hierarchical zeolite. Except for GO, the commercial hydroxyl-functionalized CNTs, which were surface modified by abundant –OH and –COOH species, favored the formation of mesoporous ZSM-5 [43]. Driven by the desire to improve the interfacial effect between the rigid substrate and zeolite precursor, the hydrophilic modifications of the template have been performed. For example, carbon black treated with NaClO could be well dispersed in the initial precursors, leading to hierarchical ZSM-5 with uniform porosity [44]. As a powerful oxidant, the HNO_3 solution was also used for the modification of carbon materials. Typically, the oxidative treatment of Merck carbon was performed by mixing with HNO_3 solution and subsequently evaporating until dryness [45]. Recently, Huang's group reported the preparation of highly efficient carbon templates by carbonization of the mixture of polythene oxide and urea. The –C–O–C– groups on the surface were transformed into –C–O–H bonds in the gel system, thereby enhancing the hydrophilicity and compatibility of the carbon templates [46]. So, it can be concluded that the surface chemical characteristics of the added carbon make a significant impact on the natural features of zeolites, such as porosity, particle size, and morphology. The hydrophilic modifications could avoid the extrusion of carbon during the growth of zeolite crystal, but this operation is accompanied by complicated routes and high economic costs. Therefore, the large-scaled production of efficient and cheap carbon templates is expected.

Three-dimensionally ordered macro/mesoporous (3DOM/3DOm) structured zeolites, which exhibit the advantages of ordered porosity, high interconnection, and superior hydrothermal stability, are of considerable interest for scientific research and industrial application. The electron microscopy and schematic illustration of ordered macro/mesoporous structured zeolites synthesized by the HTS route were shown in Fig. 1. Novel carbon materials with 3DOM/3DOm were precisely prepared. The synthesis route mainly involved three steps: the infiltration of the organic precursor into colloidal interstitial space, carbonization in flowing inert atmosphere, and removal of templates. As Yoo et al. reported [47,48], 3DOM carbon with pore size of ~350 nm was synthesized using poly (methyl methacrylate) colloidal crystals and resorcinol-formaldehyde as templates and carbon sources, respectively. Then, the surface was alternately modified with positive and negative polyelectrolytes. The charged 3DOM carbon was employed to synthesize silicalite-1 using recycled infiltration/hydrothermal method. Typically, the carbon was immersed into the zeolite solution during hydrothermal treatment. Then the seeded zeolites were recovered and re-inserted into a fresh solution to critically control the crystal growth process, and the operation was repeated several times. When the 3DOM carbon was soaked in the precursor solution with high silica concentration ($H_2O/Si = 11.4$), the monodisperse silicalite-1 spheres trapped in the cages of 3DOM carbon templates were formed (Fig. 1(a)). Contrarily, The condition of low silica concentrations ($H_2O/Si = 475$) favored the crystal growth. The growth of seeds could extend to adjacent cages of 3DOM through the window, resulting in the formation of interconnected single-crystal domains with diameters of several micrometers after five cycles (Figs. 1 (b) and 1(c)).

Subsequently, through this straightforward multiple hydrothermal treatments, 3DOm-structured zeolites could be realized [18]. The 3DOm carbon templates were prepared by filling furfuryl alcohol into the packed space of mesoscopic-sized silica colloidal. Using precursors with low silica concentration ($H_2O/Si = 405$), the 3DOm-structured zeolite single crystals were synthesized. The confined growth of zeolite in the interior space of 3DOm carbon could be achieved, which avoided the crystal formed outside. Moreover, as displayed in Fig. 1(d), further studies demonstrated that various zeolites, including those with *BEA, MFI, FAU, LTL, LTA topologies, were synthesized by this confinement effect. Based on the above research, the 3DOm ZSM-5 [49], *BEA [50], Sn-MFI [51], SAPO-34 [52], *BEA/MFI nanocomposites [53] were also successfully fabricated, indicating the feasibility of the strategy. From a scientific perspective, the confined synthesis of ordered macro/mesoporous zeolites provides a reference example for understanding the crystallization mechanism of zeolite and arouses inspiration for designing novel synthetic schemes. The precursor concentration is a decisive factor for the features of the obtained zeolites, such as porous structure and particle size. In this strategy, a lower concentration is necessary to be controlled to construct the interconnected porous structured zeolites. The three-dimensionally ordered pores endows the zeolite's interconnected structure, which makes it possible to establish a relationship between the porous structure and the performance of zeolites. However, further industrial production might be limited due to the complicated and time-consuming process.

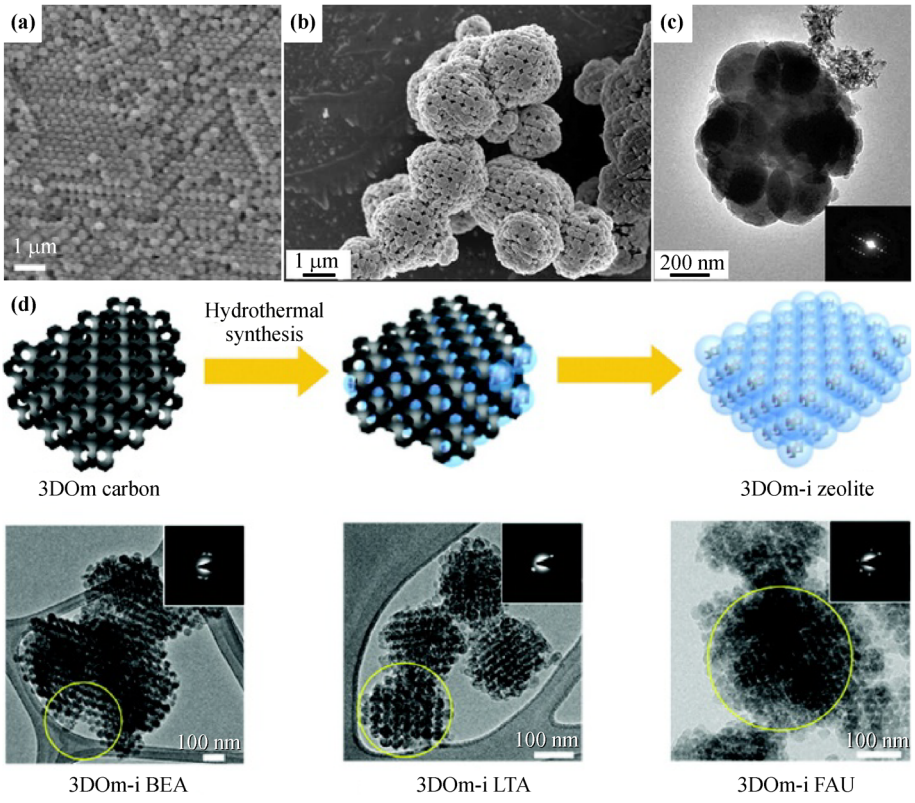

Fig. 1 Summary of zeolites using ordered porous carbon as templates via HTS process: (a) Scanning electron microscopy (SEM) image of the agglomerate of close-packed spheres with high silica concentration. Reprinted with permission from ref. [47], copyright 2008 Wiley. (b) SEM and (c) transmission electron microscopy (TEM) images of the sample obtained with low silica concentration. Reprinted with permission from ref. [48], copyright 2009 American Chemical Society. (d) Schematic illustration and TEM images of 3Dom-structured zeolites through multiple hydrothermal treatments. Reprinted with permission from ref. [18], copyright 2011 American Chemical Society.

2.2 Dry gel conversion

DGC is a technique of transforming dried precursor gel into crystal under water steam or mixed vapor of steam and volatile microporous structure-directing agent, where the precursor mixture is not directly in contact with the liquid medium. To eliminate the phase separation during hydrothermal crystallization, DGC is extensively utilized in the synthesis of carbon templated zeolites. The mass transport of the DGC process is much lower than that of the HTS method, because of the limited amount of water medium presented in the precursor gel mixture. So it is beneficial for realizing the *in situ* confined crystallization in porous channels of carbon templates, avoiding the migration of precursors from the pores networks to form separate bulk zeolites. The rational synthesis consists of three steps: 1) preparation of dried carbon-gel mixture by impregnating the precursor solution on carbon templates and subsequent aging, drying; 2) crystallization in a designed autoclave with sufficient water at the bottom; 3) combustion of carbon templates in air or O_2 flow.

Many researchers have focused on the DGC route to synthesize hierarchical zeolites for the efficient utilization of carbon templates. The TEM images of different carbon-templated zeolites were exhibited in Fig. 2. Nanosized zeolite crystals, such as silicalite-1, ZSM-5, zeolite Beta, zeolite X, and zeolite A, were synthesized by impregnating low-viscosity precursor solutions into the mesopore system of carbon black inert matrix through the DGC process [54–56]. However, with excess zeolite gel, large zeolite single crystals with intracrystal mesopores formed (Fig. 2(a)), indicating that seeded zeolite nucleated inside the mesopores and outside the templates. The carbon nanoparticles were trapped in zeolite single crystal during the crystallization, giving rise to auxiliary pores [26,57–61]. To improve the porosity of carbon nanoparticles-templated ZSM-5, desilication in NaOH solution was performed, and the porous volume of the corresponding product was increased compared with the parent sample [62]. Subsequently, to realize the accessibility of the pores, CNTs were selected as pore-forming agents [17,63]. The TEM image in Fig. 2(b) depicted that the straight channels derived from the penetration of CNTs were randomly oriented. Moreover, the sizes of the mesopores could be adjusted by controlling the diameter of CNTs. Besides, the dispersed CNTs in gel could affect the nucleation and

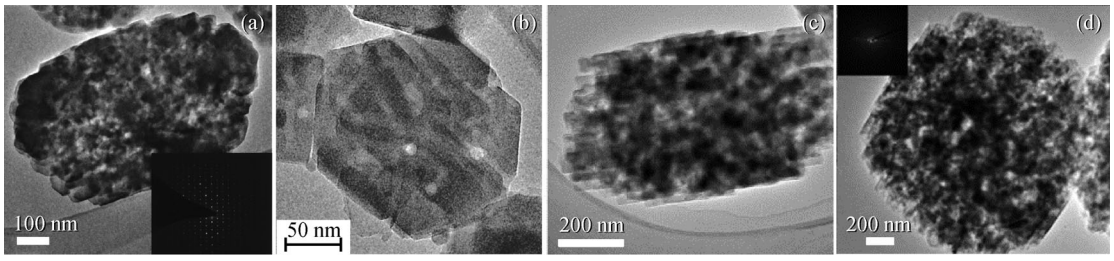

Fig. 2 Summary of TEM images of carbon templated zeolite via DGC process: (a) Hierarchical ZSM-5 using carbon black as templates. Reprinted with permission from ref. [26], copyright 2000 American Chemical Society. (b) Hierarchical silicalite-1 using CNTs as templates. Reprinted with permission from ref. [17], copyright 2001 American Chemical Society. (c) Hierarchical silicalite-1 using carbon aerogel as templates. Reprinted with permission from ref. [27], copyright 2008 Elsevier. (d) Hierarchical silicalite-1 using carbonized carbohydrates as templates. Reprinted with permission from ref. [65], copyright 2007 Wiley.

growth behaviors of zeolites, which lead to the generation of mesopores. However, it was claimed that the mesopores were not due to the space occupation of carbon. The addition of carbon modified the crystallization process and gave rise to the formation of mesopores [64]. Carbon aerogels were of great interest to the researchers, because of the three-dimensional mesoporous network and uniform size of nanoparticles. As observed in Fig. 2(c), the created pores in a zeolite particle were interconnected. Using aerogel obtained with different resorcinol to catalyst molar ratio as templates, the mesoporous size of resulting Meso-S-1 could be adjusted [27]. The tailorable pore size of the products was significant to study the effect of porosity on catalytic performance.

Considering the economic costs, inexpensive carbohydrate was employed as raw materials of carbon templates. The mesoporous carbon was available by hydrothermal treatment of widely available sucrose in ammonia solution and subsequent carbonization in an inert atmosphere. As shown in Fig. 2(d), with porous carbon as a template, ZSM-5 with abundant mesopores were synthesized [65]. The one-pot fabrication of hierarchical zeolites assisted by *in situ* generated carbon, where the crystallization of zeolite and formation of porogen took place simultaneously, was also developed [66,67]. Precursor mixture was obtained by mixing carbohydrate and zeolite gel, which was then subjected to heat treatment. In this case, the step of carbonization at high temperature was omitted, leading to time and energy savings, and the hydrothermal carbonization of carbohydrate created the porosity.

Recently, the construction of 3DOM/3DOm zeolite was also achieved via the DGC process, as shown in Fig. 3. According to the literature [47,48], the usage of polyelectrolyte modified carbon templates resulted in ordered macro/mesoporous structured zeolites with a diameter of several micrometers by recycled infiltration/hydrothermal process. However, the preparation is time-consuming and complex. In this study [68], ordered macro-mesoporous carbon (OMMC) materials with macropore sizes of ~200 nm acted as templates for synthesizing micron-sized zeolite Beta. Typically, the OMMC templates were impregnated into excess zeolite Beta precursor slurry, followed by aging, drying, and steam-assisted crystallization process. The ordered macro-mesoporous single crystals Beta were synthesized. As shown in Figs. 3(a) and 3(d), the representative Beta crystals of 1.5–2 μm were composed of many tightly intergrown zeolite spheres of 200 nm. The release of space occupied by the OMMC templates through combustion form interconnected channels inside crystalline particles. The thermal and hydrothermal stability test claimed that the well-defined frameworks with high crystallinity were intact after treatment, indicating significant potential for practical applications. Then, with OMMC as templates, the hierarchical single-crystal ZSM-5 with different Si/Al molar ratios were successfully prepared by this versatile confined crystallization process [69]. Due to the interconnected macro-meso-micropores, single-crystal nature, and high pore volume, the ZSM-5 showed higher activity and lower coking rate in cracking of bulky-molecule and methanol to olefins reaction. With the merits of interconnected porosity, universal versatility, micron-sized crystal, and simplified operation, the ordered macro-mesoporous structured zeolite is valuable for fundamental research and industrial applications.

Fan et al. also achieved the nanofabrication of zeolites with three-dimensionally ordered mesopores via DGC treatment [70]. The transparent silicalite-1 sol was immersed into the 3DOm carbon templates to ensure that the amount of SiO_2 accounted for 30 wt-% of the carbon templates. Followed by steam-assisted crystallization at high temperature, the 3DOm-structured silicalite-1 single crystal was synthesized. As shown in Figs. 3(b) and 3(e), the isolated particulate domains were composed of uniformly sized nanocrystals, which diameter was consistent with the mesopores size of the 3DOm carbon templates (~20, 30, and 40 nm). The single-crystal nature of the domain was confirmed by the representative electron diffraction pattern. Later, the fabrication of *BEA/MFI zeolite nanocomposites by overgrowing MFI crystals on

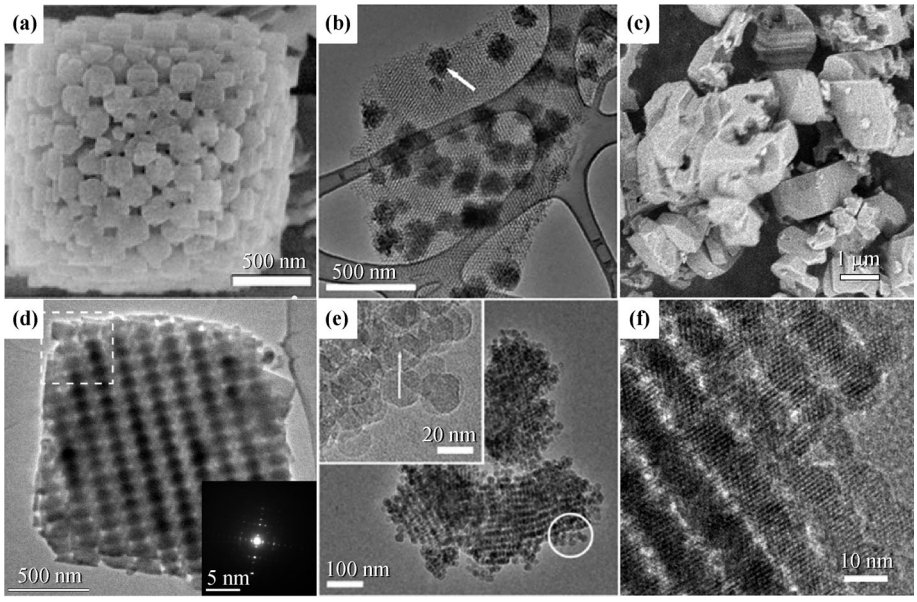

Fig. 3 Summary of three-dimensionally ordered porous structured zeolites via DGC process: (a) SEM and (d) TEM image of ordered macro-mesoporous zeolite Beta. Reprinted with permission from ref. [68], copyright 2020 Wiley. (b, e) TEM images of 3DOm carbon templated silicalite-1 single crystals. Reprinted with permission from ref. [70] copyright 2008 Nature. (c) SEM image and (f) TEM image of CMK-L templated silicalite-1 crystals. Reprinted with permission from ref. [29], copyright 2011 Elsevier.

3DOm-structured *BEA was reported [53]. First, 3DOm-structured *BEA zeolite with 35 nm nanocrystalline grew in the confined space provided by carbon templates. Then 3DOm-structured *BEA was impregnated with MFI precursor sol. Finally, through dry gel transformation, zeolite nanocomposites with different micropore frameworks were generated. However, as indicated in characterization, the isolated particles with the size of about 100–300 nm belonged to the category of nano-sized zeolite, which resulted in difficult separation. More importantly, the utilization efficiency of 3DOm-structured carbon was not satisfactory because part of the template was not involved in directing crystallization of mesoporous zeolites (Fig. 3(b)).

CMK-type carbon materials were delicate replications of ordered mesoporous silica with different topologies and pore structures [71,72], which were used to template ordered mesopore structure in the zeolite. In fact, it is challenging to crystalize the gel in the confined mesoporous channels because of the incompatibility between the narrow channels (several nanometers) and structural units of zeolites. Surprisingly, Ryoo's groups reported a successful attempt to replicate CMK-type materials into ordered mesoporous zeolites under steaming condition [29]. In this research, CMK-L with 10 nm pore diameters and 5.1 nm wall thickness was chosen as a rigid template derived from mesoporous silica KIT-6. As illustrated in Figs. 3(c) and 3(f), under optimum humidity, the MFI zeolites with preserved ordered mesopores and fully crystallized walls were synthesized. The relative humidity, channel diameter, and framework rigidity of the template were all the keys to precisely control the crystallization in the mesopore network. This work provided the guiding significance for the synthesis of ordered mesoporous zeolites from the aspects of the selection of porous carbon templates and the determination of crystallization conditions.

In summarizing the literature, significant progress has been made in the synthesis of hierarchical zeolites by the direct templates method. The summary of carbon-templated zeolites by HTS and DGC process was listed in Table 1. The characteristics of zeolites, such as morphology, size, and porous structure, are strongly related to the nature of carbon templates and the selection of crystallization approach. The HTS approach which exhibits advantages, such as versatility of different zeolites and simplicity of operation, were versatile for fabricating different zeolites, but it is limited by the severe phase separation and low utilization of carbon templates. The advantages of the DGC are its low consumption of solvents and efficient utilization of carbon, while the disadvantages of this approach include the requirement of designed devices and a limited list of available zeolites.

3 Indirect templates

In contrast to the syntheses accomplished by mixing additional carbon templates into the zeolite precursor mixture, impregnating the C-Si composites, which formed by carbonization process, into the microporous structure-directing agent for zeolitization was developed. In this case, the composites were used as both Si precursors and pore-generating agents. Due to the enhanced affinity

Table 1 Summary of hierarchically mesoporous zeolite synthesized by additional carbon templates [a)]

Zeolite	Carbon template	Gel composition molar ratio	Crystallization approach (temperature/°C, time/d)	$V_{macro/meso}$/ ($cm^3 \cdot g^{-1}$)	Macro/mesopore size/nm	Model reaction	Porous characteristic	Ref.
ZSM-12	Carbon nanoparticle	1 Na_2O:1 Al_2O_3:150 SiO_2:36 TEAOH:4500 H_2O:150 C	HTS (160, 9.5)	0.15–0.19	10–50	Conversion of *n*-tridecane; 1,3-dimethylcyclohexane	Meso-micropores; intracrystal and disordered	[30]
MCM-22	Carbon nanoparticle	9.25 NaOH:4.51 $NaAlO_2$:4.51 H_2O:50.21 HMI:100 SiO_2:4.95 C	HTS (135, 7)	0.44	200	–	Macro-meso-micropores; intercrystal, disordered and interconnected	[31]
SAPO-34	Carbon nanoparticle	1.0 Al_2O_3:1.0 P_2O_5:0.6 SiO_2:1.5 MOR:0.5 TEAOH:60 H_2O:13.5 C	HTS (180, 2)	0.456	–	Uptake of *n*-butane; methanol to olefin	Intracrystal and disordered	[32]
SAPO-34	CNT	1.0 Al_2O_3:1.0 P_2O_5:0.6 SiO_2:1.5 MOR:0.5 TEAOH:60 H_2O:13.5 C	HTS (180, 2)	0.364	–	Uptake of *n*-butane; methanol to olefin	Intracrystal, disordered and interconnected	[32]
ZSM-5	CNT	1.00/0.50/0.33 Al_2O_3:10 TPABr:10 Na_2O:40 SiO_2:7200 H_2O:647 C	HTS (175, 3)	–	20–50	Hydroconversion of soybean oil	Meso-micropores; intracrystal, disordered and interconnected	[33]
SAPO-34	CNT	1 Al_2O_3:1 P_2O_5:*x* TEAOH:(2 − *x*) MOR:60 H_2O:(0–10.2) C, *x* = 0.0, 1.0, 2.0	HTS (190, 1)	0.175–0.516	–	Methanol to olefin	Intracrystal and disordered	[34]
Beta	CNT	2.69 Na_2O: 1 Al_2O_3:50.76 SiO_2:12.68 TEAOH:810.24 H_2O (2.8 g C/gel)	HTS (170, 1)	0.27	25	Hydrocracking of vacuum gas-oil	Meso-micropores; disordered	[35]
NaY	Carbon aerogel	1.00 Al_2O_3:4.35 SiO_2:2.39 $(TMA)_2O$:0.065 Na_2O:248.00 H_2O	HTS (100, 9)	1.37	10	–	Meso-micropores; disordered	[37]
ZSM-5	Carbon aerogel	10 Na_2O:200 SiO_2: 1 Al_2O_3:20 TPABr:1600 H_2O	HTS (100, 9)	0.2	11	–	Meso-micropores; intercrystal, disordered and interconnected	[38]
ZSM-5	Biomass-derived carbon	30.5 H_2O:0.017 $Al(OC_4H_9)_3$: 1 $Si(OC_2H_5)_4$: 1 TPAOH	HTS (160, 3)	0.13	12–16	–	Meso-micropores; intracrystal, disordered and interconnected	[39]
Beta	GO	1.5 Na_2O:Al_2O_3:40 SiO_2:10 TEAOH:532 H_2O:(4–20) C	HTS (140, 4–32)	0.12–0.20	3–7	–	Meso-micropores; intercrystal and disordered	[28]
ZSM-5	Hydroxylated CNT	100 SiO_2: 1 Al_2O_3: 1 Na_2O:0.2 $(TPA)_2O$:17 H_2O:72 C	HTS (180, 3)	0.14	10–35	Cracking of *tri*-isopropylbenzene	Meso-micropores; intracrystal and disordered	[43]
ZSM-5	Carbon black oxidized by NaClO	80 SiO_2:Al_2O_3:7 TPA_2O:1775 H_2O:160400 C	HTS (170, 2)	0.13–0.17	5–18	Disproportionation of toluene	Meso-micropores; intracrystal and disordered	[44]
ZSM-58	CNT oxidized by HNO_3	21 MTI:100 SiO_2:1 Al_2O_3:3056 H_2O:12 NaOH	HTS (160, 5)	0.06	3–20	Selective adsorption of propene over propane	Meso-micropores; intracrystal and disordered	[36]
SAPO-11	Merck carbon oxidized by HNO_3	1.0 Al_2O_3:1.0 P_2O_5:0.4 SiO_2:1.5 DPA:50 H_2O (0.06 g C/gel)	HTS (200, 1)	0.10	–	Hydroisomerization of *n*-decane	Disordered	[45]
ZSM-5	Carbon nanoparticle	2 Al_2O_3:20 TPA_2O:1 Na_2O:100 SiO_2:200 H_2O	HTS (180, 3)	0.45	34.5	Benzylation of mesitylene with benzyl alcohol	Meso-micropores; intracrystal and disordered	[46]
Beta	3D CMK-n	25 SiO_2:0.25 Al_2O_3:4.5 $(TEA)_2O$:0.35 Na_2O:330 H_2O:66.9 C	HTS (100, 4) repeated 4 times	0.3–0.58	–	–	Meso-micropores; intracrystal, ordered and interconnected	[18]

(*Continued*)

Zeolite	Carbon template	Gel composition molar ratio	Crystallization approach (temperature/°C, time/d)	$V_{macro/meso}$/ ($cm^3 \cdot g^{-1}$)	Macro/mesopore size/nm	Model reaction	Porous characteristic	Ref.
LTA	3D CMK-n	11.25 SiO_2:1.8 Al_2O_3:13.4 $(TMA)_2O$:0.6 Na_2O:700 H_2O:6.75 C	HTS (70, 0.5) repeated 6 times	0.28–0.68	–	–	Meso-micropores; intracrystal, ordered and interconnected	[18]
FAU	3D CMK-n	10 SiO_2:2.3 Al_2O_3:5.5 $(TMA)_2O$:1.2 Na_2O:570 H_2O:6.22 C	HTS (100, 4) repeated 5 times	0.29	–	–	Meso-micropores; intracrystal, ordered and interconnected	[18]
Sn-MFI	3D CMK-n	1 SiO_2:0.008 SnO_2:0.43 TPAOH:22.20 H_2O:1.5 C	HTS (170, 1) repeated 3 times	0.283	4–11	Isomerization of cellulosic sugars	Meso-micropores; intracrystal, ordered and interconnected	[51]
SAPO-34	3D CMK-n	0.6 SiO_2:2 TEA_2O:Al_2O_3:2 P_2O_5:75 H_2O:2.92 $Al(OPri)_3$:0.189 C	HTS (180, 0.83) repeated 5 times	0.23–0.33	5.5–13	Methanol to olefin	Meso-micropores; intracrystal, ordered and interconnected	[52]
ZSM-11	Carbon nanoparticle	1 Al_2O_3:100 SiO_2:20 TBA_2O:1 Na_2O:200 H_2O:900 C	DGC (180, 3)	0.40	–	Cracking and isomerization of *n*-hexadecane	Intracrystal and disordered	[59]
TS-2	Carbon nanoparticle	1 TiO_2:100 SiO_2:20 TBA_2O:200 H_2O:900 C	DGC (180, 3)	031/0.44	–	Epoxidation of oct-1-ene and styrene	Intracrystal and disordered	[59]
ZSM-5	Carbon nanoparticle	1 Al_2O_3:100 SiO_2:20 TPA_2O:1 Na_2O:200 H_2O:900 C	DGC (180, 3)	0.40	–	Direct NO decomposition	Intracrystal and disordered	[60]
TS-1	Carbon nanoparticle	5 TBOT:312 TEOS:123 TPAOH:9722 H_2O:223 $C_4H_{10}O$:4159 C	DGC (175, 1)	0.26	20–50	Hydroxylation of phenol and ammoxidation of methyl-ethyl ketone	Meso-micropores; intracrystal and disordered	[61]
SAPO-34	CNT	1 Al_2O_3:1 P_2O_5:0.6 SiO_2:6 DEA:70 H_2O:0.9 C	DGC (200, 6)	0.031	0–50	Methanol to olefin	Meso-micropores; intracrystal and disordered	[63]
Beta	OMMC	1 TEOS:1 TPAOH:0.04 $Al(OC_3H_7)_3$	DGC (180, 3)	0.18	40	Liquid-phase Friedel-Crafts alkylation of benzene with benzyl alcohol	Marco-meso-micropores; intracrystal, ordered and interconnected	[68]
ZSM-5	OMMC	0.36 TPAOH:SiO_2:*x* Al_2O_3:19.2 H_2O (*x* = 0.067, 0.040, 0.020)	DGC (180, 3)	–	35	Cracking of bulky 1,3,5-TIPB; methanol to olefin	Marco-meso-micropores; intracrystal, ordered and interconnected	[69]
Silicalite-1	3DOm	9 TPA_2O:0.15 Na_2O:50 SiO_2:390 H_2O:180 ethanol	DGC (180, 2)	0.69–0.99	6	–	Meso-micropores; intracrystal, ordered and interconnected	[70]
Silicalite-1	CMK-L	(0–2) $Al(OC_3H_7)_3$:25 TPAOH:100 TEOS	DGC (170, 6)	0.17	8.7	–	Meso-micropores; intracrystal, ordered and interconnected	[29]

a) TEAOH: tetraethyl ammonium hydroxide; HMI: hexamethyleneimine; TPABr: tetrapropylammonium bromide; TPAOH: tetrapropyl ammonium hydroxide; DPA: diphenylamine; TBOT: tetrabutyl titanate; DEA: diethanolamine; TEOS: tetraethyl orthosilicate; 1,3,5-TIPB: 1,3,5-triisopropylbenzene.

between silica and carbon template in the composite, the templating effect of carbon could be fully exploited. In this section, according to the porous structure and preparation method, different composites were further classified into CMK-n-silica composites, carbon-coated silica composites, and carbon-silica monolithic composites. The electron micrographs of obtained hierarchical zeolites were shown in Fig. 4 (cf. Section 3.3).

3.1 CMK-n-silica composites

To synergize the advantages of the ordered mesoporosity and unique acidity of zeolites, *in situ* crystallization of the ordered mesoporous materials synthesized by the surfactants template method was performed. To prevent the collapse of periodic mesostructure, the ordered mesoporous silica-CMK typed composites were formed by the carbonization of filled organic species or surfactants in the mesopore channels. Carbonaceous CMK-n served as the stabilizer to support the silica framework during crystallization. According to previous researches, the complete conversion of pore wall into microporous crystalline has not been realized. In most cases, the generation of mesoporous materials with deposited zeolite frameworks has been proved [73,74]. The silicalite-1/SBA-15 composite was obtained by crystallizing the carbon-filled SBA-15 through solid-phase transformation and the short-ranged crystal domains were embedded inside the mesoporous SBA-15 matrix [75]. Moreover, the partially crystallized composites were of great interest for industrial purposes as the improved diffusion and zeolitic characteristics. However, it is challenging to obtain ordered mesoporous zeolites with the completely crystallized mesoporous wall because the poorly thin wall is not rigid enough to hold zeolite building units. With the prolonged crystallization time, the ordered mesoporous silica-CMK-n composites were completely crystallized into mesoporous zeolites without mesostructured periodicity [76,77]. The CMK-n materials were wrapped in zeolites particles and served as templates of auxiliary porosity during the crystallization. In this zeolitization transformation process, the ordered mesopores walls of silica were unstable and completely collapsed, so the advantages of the ordered mesostructure were not preserved and utilized.

CMK-n-silica nanocomposites were also synthesized by the nonionic triblock copolymer templating method. Through the co-assembly of the silica precursors, carbon precursors, and mesomorphous micelles of surfactant, the composites with meso-channel walls consisted of carbon and silica were generated. During the crystallization of the CMK-n-silica nanocomposites, the inter-embedded carbon in the composites framework could impede the growth and aggregation of generated zeolite seeds. So, in this case, some domains did not convert into microporous zeolite because of the locking effect of carbon species. Careful control of the moderate crystallization condition should be made to yield the complex with a partially maintained mesostructured framework and microcrystalline units [78–80]. As displayed in SEM and TEM images (Figs. 4(a) and 4(e)), hierarchical ZSM-5 zeolites were constructed, and each particle was composed of linked microcrystalline units [81]. The CMK-n-silica composites with intergrowth pore walls tended to form partially crystallized zeolites framework due to the confined effect of carbon.

3.2 Carbon-coated silica composites

The carbon-coated silica composites were produced by immersing silica with the required amount of organic carbon precursor, such as sucrose, dopamine, and

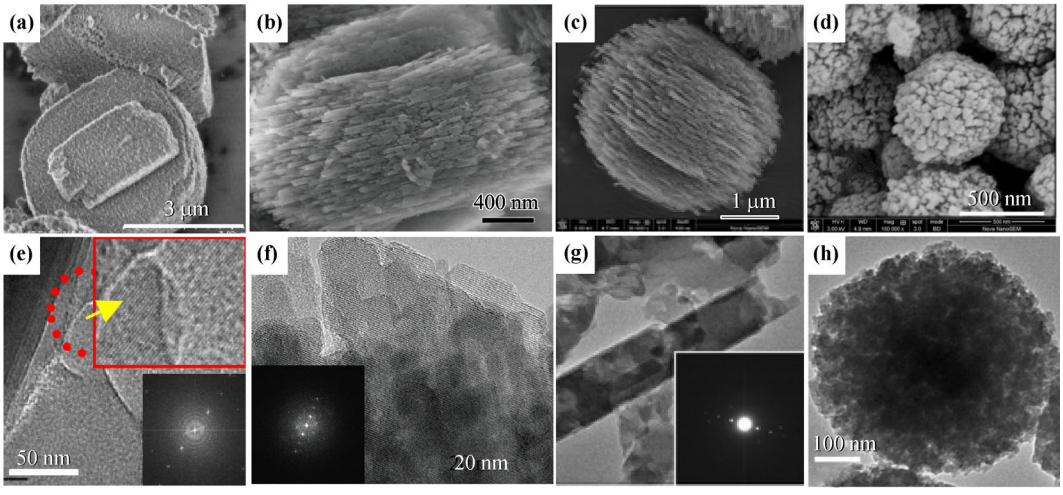

Fig. 4 Summary of hierarchical zeolites derived from carbon-silica composites. Top: SEM images. Bottom: TEM images. (a, e) ZSM-5 zeolite. Reprinted with permission from ref. [81], copyright 2020 Wiley. (b, f) Silicalite-1 zeolite. Reprinted with permission from ref. [85], copyright 2018 Royal Society of Chemistry. (c, g) Silicalite-1 zeolite. Reprinted with permission from ref. [91], copyright 2013 Royal Society of Chemistry. (d, h) Zeolite Beta. Reprinted with permission from ref. [92], copyright 2016 Elsevier.

subsequent carbonization. The deposited carbon layer on the surface of silica served as the sacrificial template for generating auxiliary pores. During the crystallization, the carbon template trapped in crystal particles leads to pores [82–84]. Furthermore, the "wall" effect of the carbon layer to confine the overgrowth of zeolite nanocrystals was demonstrated. As reported [85,86], by steam-assisted crystallization, core-shell structured carbon-silica composites converted into meso-microporous MFI-type zeolites, which were packed by numerous interlinked nanocrystals. As shown in Figs. 4(b) and 4(f), the size of nanocrystals was close to that of added silica sphere, which proved the effect of carbon shell on restricting the epitaxial growth of zeolite.

Another direct deposition method to prepare carbon-coated silica composites by decomposing and depositing carbonaceous gases on the surface of silica was developed, thereby simplifying the operation procedures. Silica spheres were subjected to the heating treatment of carbonaceous gas flow, such as methane, acetylene, and propane. Varying the gas concentration and deposition time, the composites with different coke/silica ratios could be yielded, which were used to adjust the porosity of zeolites [87–90]. The advantages of this approach are its simplicity and controllability of the porosity. However, it is limited by the consumption of expensive hydrocarbon gas and the safety issues in the carbonization process.

3.3 Carbon-silica monolithic composites

Great attention is also paid to zeolite synthesis by adopting carbon-silica monolithic composites as raw materials. The carbon-silica monolith with the component of 40 wt-% carbon and 60 wt-% SiO_2 were hydrothermally prepared with carbohydrate, polymerized resin, and tetraethyl orthosilicate as raw materials. Using that as the precursor, single-crystal MFI-type zeolite microspheres with 5–10 um diameter was yielded (Figs. 4(c) and 4(g)). The percent of carbon had a significant influence on the formation of microspherical structures. With the features of micron-scaled crystal size, simple preparation process, and interconnected pores, zeolite microspheres showed great potential for practical application [91]. Hierarchically porous zeolite Beta was synthesized by impregnating the zeolites Beta sol into the carbon-silica monolith. The resultant Beta zeolites were spherical aggregates made of stacked nanoparticles (Figs. 4(d) and 4(h)), and the voids of nanoparticles formed the hierarchical pores inside crystals [92].

In the above research, the morphology and particle size of carbon-silica raw materials were not preserved during crystallization. According to the mechanism of zeolite crystallization, precursor species dissolve in alkaline solution to form a gel and then convert into crystalline particles. So it is challenging to achieve *in situ* crystallization without migration of Si species. Huang et al. [93] described a confined space approach to synthesize tailorable sized zeolite NaA using colloidal silica with the average size of 100 nm as a SiO_2 source. With the presence of Pluronic P123, furfuryl alcohol self-polymerized on the surface of SiO_2 to produce the silica-P123-furfuryl alcohol monolith. To prevent silica from penetrating outside the composites, surface coating of the monolith was further performed with polymerization of FA. The silica-P123-furfuryl alcohol complex was heat-treated at 500 °C in N_2 flow, leading to the produce of carbon-silica monolithic composites with porous carbon coating. Then, the penetration of alkaline zeolite NaA solution and hydrothermal crystallization was carried out. In this study, partial silica spheres embedded in porous carbon monolith were in situ converted into NaA zeolite without change of morphology and size. Much effort is worthwhile in this field, which involves the study of crystallization mechanism, and provides guiding significance for the construction of zeolites.

Monolithic zeolite with a hierarchically porous structure of interconnected macro/mesopore and micropore is promising in diverse high throughput or requiring low pressure drop processes. The carbon templating method as a simple and general procedure has been established to fabricate such zeolite monolith with pore hierarchy. Hierarchically porous ZSM-5 monolith with 2 cm diameter $\times$ 5 mm thick obtained by the crystallization of SBA-15 containing carbon in the pores with the induce of TPAOH. Similarly, the ZSM-5 crystal films deposited on the glass were also successfully obtained [94]. What's more, various shaped zeolite Beta monoliths could be easily synthesized by converting carbon-containing silica molded in different shapes via hydrothermal crystallization [95]. With the production of monolithic zeolite, the shaping procedure of the catalyst could be omitted in the application process. The mass transport and accessibility of active sites were improved with the introduction of hierarchical pores, so the carbon templated zeolite monolith is an exciting catalyst material and deserves more attention in the future.

In summarizing the literature, hierarchical zeolites were successfully fabricated through the indirect template method. The summary of the indirect templated zeolites was listed in Table 2. Compared to the direct templates methods, the highly efficient utilization of carbon templates was realized due to the enhanced interaction between carbon and silica. However, the complex of amorphous and crystallized phase easily formed during this process, which could be overcome by prolonging the crystallization time.

4 Fixation of metal nanoparticles into hierarchical zeolites

Fixation of transition metal or noble metal species into the zeolitic framework, could further extend the performance

Table 2 Summary of the crystallization of carbon-silica composites [a)]

Composites	Carbon source	Structure-directing agent	Crystallization approach (temperature/°C, time/d)	Product	$V_{macro/meso}$/($cm^3 \cdot g^{-1}$)	Pore size /nm	Model reaction	Porous characteristics	Ref.
Al-SBA-15/CMK-3	Furfuryl alcohol	Ethylenediamine and triethylamine	DGC (175, 3)	Mesoporous materials with MFI zeolitic characteristics	–	9.0	Cracking of cumene	Meso-micropores; ordered	[73]
SBA-15/CMK-3	Furfuryl alcohol	TPAOH	SPT (130, 2)	Silicalite-1/SBA-15 composite	0.26	6	–	Meso-micropores; ordered	[75]
SBA-15/CMK-3	P123	TPABr	HTS (180, 2)	Mesoporous ZSM-5	0.26/0.32	20–40	Methanol to propylene	Meso-micropores; ordered and interconnected	[76]
SiO_2-TiO_2/C	Tween-40	TPAOH	HTS (180, 1)	Mesoporous TS-1	0.29	2–95	Oxidative desulfurization	Macro-meso-micropores; intracrystal and interconnected	[77]
P127 templated SiO_2/C composite	Phenol-formaldehyde resin	TPAOH	DGC (130, 3)	Mesoporous materials with silicalite-1 nanocrystal	0.43	7	–	Meso-micropores; ordered	[78]
P127 templated SiO_2/C composite	Phenol-formaldehyde resin	TPAOH	DGC (130, 3)	Mesoporous materials with ZSM-5 nanocrystal	0.32	9	–	Meso-micropores; ordered	[78]
P123 templated SiO_2/C composite	Furfuryl alcohol	TPAOH	DGC (140, 0.5)	ZSM-5 zeolites composed of linked microcrystalline units	0.35	6–8	Benzylation reaction between naphthalene and benzyl chloride	Meso-micropores	[81]
C deposited SiO_2	Sucrose	TBAOH	HTS (180, 3)	Mesoporous ZSM-11	0.04	–	–	Intracrystal and disordered	[82]
C deposited SiO_2-TiO_2	Sucrose	TPABr	HTS (170, 7)	Mesoporous TS-1	0.10–0.42	5–90	Oxidative desulfurization	Macro-meso-micropores; Intracrystal, disordered and interconnected	[83]
C coated SiO_2	Sucrose	TPAOH	HTS (160, 1)	Mesoporous silicalite-1	0.197	9.4	–	Meso-micropores; intercrystal and disordered	[84]
C coated SiO_2	Sucrose	TPAOH	HTS (160, 1)	Mesoporous ZSM-5	0.263	7.7	Adsorption of methylene blue, acetalization of cyclohexanone	Meso-micropores; intercrystal and disordered	[84]
C coated SiO_2	Dopamine	TPAOH	DGC (180, 0.42)	Mesoporous ZSM-5	–	4–10	Cracking of isopropyl benzene	Meso-micropores; intracrystal, disordered and interconnected	[85]
C coated SiO_2	Dopamine	TPAOH	DGC (180, 0.5)	Mesoporous ZSM-5	0.13–0.34	18	Self-etherification of benzyl alcohol	Meso-micropores; intracrystal, disordered and interconnected	[86]

(*Continued*)

Composites	Carbon source	Structure-directing agent	Crystallization approach (temperature/°C, time/d)	Product	$V_{macro/meso}$/ ($cm^3 \cdot g^{-1}$)	Pore size /nm	Model reaction	Porous characteristics	Ref.
C deposited SiO_2	CH_4 flow	TBAOH	DGC (175, 1)	Mesoporous ZSM-11	0.28	6–30	–	Meso-micropores; intracrystal and disordered	[87]
C deposited SiO_2	CH_4 flow	TEAOH	DGC (140, 6)	Mesoporous Beta	0.26	7–30	–	Meso-micropores; intracrystal and disordered	[87]
C deposited SiO_2	CH_4 flow	Seed	DGC (100, 0.75)	Mesoporous Y	0.02	10–40	–	Meso-micropores; intracrystal and disordered	[87]
C deposited SiO_2	CH_4 flow	TPAOH	DGC (180, 3)	Mesoporous ZSM-5	0.28–0.48	10–40	Cracking and isomerization of *n*-octane	Meso-micropores; intracrystal and disordered	[88]
C deposited SiO_2	Carbonaceous gas (C_xH_y)	TPAOH	HTS (180, 3)	Mesoporous ZSM-5	0.51–0.85	11	–	Meso-micropores; intercrystal and disordered	[89]
SiO_2/C monolith	Glucose and resorcinol	TPAOH	HTS (160, 4)	Mesoporous silicalite-1	0.27	30	–	Meso-micropores; intercrystal and disordered	[91]
SiO_2-Al_2O_3/C monolith	Glucose and resorcinol	TPAOH	HTS (160, 4)	Mesoporous ZSM-5	0.29	30	Condensation of benzaldehyde with *n*-butyl alcohol; alkylation of toluene with benzyl chloride; alkylation of toluene with benzyl chloride	Meso-micropores; intercrystal and disordered	[91]
SiO_2-TiO_2/C monolith	Glucose and resorcinol	TPAOH	HTS (160, 4)	Mesoporous TS-1	0.26	30	Hydroxylation of phenol	Meso-micropores; intercrystal and disordered	[91]
SiO_2-Al_2O_3/C monolith	Glucose and resorcinol	TEAOH	DGC (150, 5)	Mesoporous Beta	0.27	30	Dehydration of fructose into 5-hydroxymethylfurfural	Meso-micropores; intracrystal and disordered	[92]
SBA-15/CMK-3	Phenol resin	TPAOH	DGC (170, 1)	Mesoporous ZSM-5	–	10–15	Cracking of triisopropylbenzene	Meso-micropores; disordered	[94]

a) SPT: solid phase transformation; TBAOH: tetrabutylammonium hydroxide.

of hierarchically porous zeolites. Hierarchically porous zeolites loaded with metal species, combining the advantages of shape selectivity of micropores, mass transport of auxiliary pores, and catalytic activity of metal active sites, presented excellent catalytic performance in various processes. Currently, recognized strategies to prepare metal@zeolite catalysts typically include ion exchange [96,97], incipient impregnation [98,99], and *in situ* encapsulation approach [100,101]. Ion exchange is restricted by the amount of Brønsted acidic sites, hydrophilic/hydrophobic property, and pore size of zeolites. The incipient impregnation method suffers from inhomogeneity, low dispersion, and severe aggregation. To inhibit fast precipitation of metal precursors in alkaline synthetic gel, expensive organic ligands, for example, ethylenediamine, mercaptosilane, are required in reported in situ encapsulation of metal species into zeolite framework. Hierarchical porous channel of zeolites significantly improves the mass transport, accessibility of active sites, and sintering resistance of the catalyst. So, it is desirable to develop an approach with low economic cost and wide versatility for immobilizing metal nanoparticles into the internal voids of hierarchically porous zeolites.

With the addition of carbon solid templates and metal sources into the zeolite precursor solution, simultaneously, the metal-containing hierarchical zeolites would be afforded after crystallization. A series of successive impregnations of the different zeolite precursors into carbon matrix BP 2000 was conducted to form the Co-$AlPO_4$ mixture. The obtained micron-sized hierarchical CoAlPO-5 stacked with numbers elongated-shaped nanoparticles possessed both intra- and intercrystalline pores [102]. Applying the multiple hydrothermal crystallization method reported in previous literature, Cho et al. described the synthesis of hierarchical Sn-MFI with the addition of $SnCl_4 \cdot 5H_2O$ using 3DOm carbon as templates [51]. More directly, the metal salts, such as $Ni(NO_3)_2$, $Co(NO_3)_2$, and CNTs were sequentially added to the final zeolite gel. The hierarchical MeSAPO-34 (Me = Co, Ni) with embedded metal particles was successfully synthesized [103].

A more efficient method was proposed to realize the fixation of metal species into the zeolite framework. By depositing metal species on the surface of carbon templates, the strategy of one-pot synthesis of metal-supported hierarchically porous zeolites was demonstrated. Take the synthesis of Co-ZSM-5 zeolite as an example to introduce the preparation process in detail. Before the synthesis of Co-ZSM-5, the CNTs templates were impregnated into cobaltous nitrate solution and calcined in N_2 flow at 400 °C. The obtained Co/CNTs were placed into ZSM-5 zeolite sol as sacrificial templates and metal sources. Through hydrothermal crystallization, the Co/ZSM-5 porous composites with encapsulated CoO were produced [104]. Based on the above research, different metal species, such as Mg, Ni, were incorporated into ZSM-5 zeolites to expand the further application of zeolite in the fields of catalysis, adsorption, and biomedical science [105]. By the hydrothermal carbonization of cellulose and $Fe(NO_3)_3$, the Fe nanoparticles fixed in the carbon sphere were prepared as precursors for the fabrication of zeolite Y microcrystals with embedded Fe species [106]. The steam-assisted crystallization was also deployed to synthesize metal-containing hierarchical zeolites. The hierarchical Ga/ZSM-5 composed of assembled nanounits and Ga_2O_3 nanoparticles were obtained by adopting a similar procedure [107]. What's more, the location of Ga species in Ga-CNTs composites significantly impacted the properties of the Ga-loaded MFI zeolites [108].

The migration and sintering of metal species, which lead to the loss of activity, could be overcome by the fixation of the nanoparticles into hierarchical zeolites. With the assistance of carbon templates, the facile formation of the hierarchical zeolites with encapsulated metal species was realized by the one-pot synthesis process, exhibiting the promising potential for use. Moreover, for wide application, this approach is required to be generally applicable in syntheses with different metal species, carbon templates, and targeting zeolite structures.

5 Conclusions and perspectives

In conclusion, hierarchically porous zeolites with characteristics of integrating macro/mesopores into the microporous framework are readily available by the carbon templating method. With the advantages of controlled generation of porosity, wide versatility, and low cost, the carbon-templating process is the most promising strategy to fabricate hierarchical zeolites with different architecture and compositions on an industrial scale. Based on the above summary and discussion, the following issues are essential for carbon templating synthesis: 1) Interaction between carbon matrix and zeolite precursor/framework. In addition to spatial confinement, chemical interaction between carbon and zeolite precursor/framework also exits in the synthetic system, which determines whether the carbon matrices can be implanted into product crystals or not. By altering the hydrophilic/hydrophobic properties of inert carbon surface, the interfacial effects can be improved, which is beneficial for achieving the efficient utilization of template by occupying more voids space inside crystals. Compared with zeolites synthesized by additional carbon templates, the crystallization of carbon-silica composites tends to form zeolites with more abundant pores. 2) Nature of carbon templates. The texture properties of zeolites are undoubtedly affected by the characteristics of carbon templates, such as the addition amount, morphology, particle size, and pore structure. Remarkably, the regularity and interconnection of the porous tunnels of produced zeolite mainly depend on the structure of templates, because it is usually a model

replication process, where introduced pores were derived from the release of encapsulated carbon by combustion. As the amount of added template increase, more carbon matrices are implanted into crystals, giving rise to the rise of the pore space. 3) Selection of crystallization approach. Adopting different crystallization methods, the crystallization kinetics and mechanism are different, significantly affecting the growth process and final structure of zeolites. Compared with traditional HTS, mass transport is much slower under stream conditions in the DGC process. So, the phase separation can be eliminated to some extent, which is favorable for the encapsulation of carbon into zeolite bodies. 4) Control of zeolite gel components. Besides the templates, the composition of zeolite gel, such as precursor source, concentration, and Si/Al molar ratio, also need to be specially modulated. The alkalinity, viscosity, and chemical property of the precursor solution can be altered with different amounts of Al source, leading to differentiated interaction between templates and gel.

Hierarchically porous zeolites are desirable materials for industrial applications, and significant progress has been achieved in the synthesis of carbon templated zeolites. With the need for large-scale production, it is highly desirable to develop a simple method to effectively improve the utilization of carbon and precisely control the interconnectivity of the pores. From a scientific point, very little progress has been accomplished in the in situ crystallization of carbon-silica composites, where the morphology and size of raw materials were maintained. The effort is worthwhile in this respect because it is beneficial for researching the crystallization mechanism of zeolites. Besides, with the potential in industrial applications, the development of synthetic strategy of the monolithic zeolite catalyst is expected. For carbon templating synthesis, the crucial role of carbon as well as interaction between carbon matrix and zeolite precursor/framework still needs further experimental verification and detailed characterization.

Acknowledgements This work was supported by the National Natural Science Foundation of China (Grant No. 21773128).

References

1. Chen L H, Sun M H, Wang Z, Yang W M, Xie Z K, Su B L. Hierarchically structured zeolites: from design to application. Chemical Reviews, 2020, 120(20): 11194–11294
2. de Jong K P, Zečević J, Friedrich H, de Jongh P E, Bulut M, van Donk S, Kenmogne R, Finiels A, Hulea V, Fajula F. Zeolite Y crystals with trimodal porosity as ideal hydrocracking catalysts. Angewandte Chemie International Edition, 2010, 49(52): 10074–10078
3. Fu T J, Qi R Y, Wan W L, Shao J, Wen J Z, Li Z. Fabrication of hollow mesoporous nanosized ZSM-5 catalyst with superior methanol-to-hydrocarbons performance by controllable desilication. ChemCatChem, 2017, 9(22): 4212–4224
4. Fang Y H, Yang F, He X, Zhu X D. Dealumination and desilication for Al-rich HZSM-5 zeolite via steam-alkaline treatment and its application in methanol aromatization. Frontiers of Chemical Science and Engineering, 2019, 13(3): 543–553
5. Yang S T, Yu C X, Yu L L, Miao S, Zou M M, Jin C Z, Zhang D Z, Xu L Y, Huang S J. Bridging dealumination and desilication for the synthesis of hierarchical MFI zeolites. Angewandte Chemie International Edition, 2017, 56(41): 12553–12556
6. Li Q, Dou T, Zhang Y, Li Y P, Wang S, Sun F M. Synthesis, characterization and catalytic properties of mesoporous MCM-48 containing zeolite secondary building units. Frontiers of Chemical Science and Engineering, 2007, 1(1): 1–5
7. Zhang W M, Ming W X, Hu S F, Qin B, Ma J H, Li R F. A feasible one-step synthesis of hierarchical zeolite Beta with uniform nanocrystals via CTAB. Materials (Basel), 2018, 11(5): 651–662
8. Du S T, Li F, Sun Q M, Wang N, Jia M J, Yu J H. A green surfactant-assisted synthesis of hierarchical TS-1 zeolites with excellent catalytic properties for oxidative desulfurization. Chemical Communications (Cambridge), 2016, 52(16): 3368–3371
9. Xu H, Lei C, Wu Q M, Zhu Q Y, Meng X J, Dai D, Maurer S, Parvulescu A N, Müller U, Xiao F S. Organosilane surfactant-assisted synthesis of mesoporous SSZ-39 zeolite with enhanced catalytic performance in the methanol-to-olefins reaction. Frontiers of Chemical Science and Engineering, 2020, 14(2): 267–274
10. Xu S M, Zhang X X, Cheng D G, Chen F Q, Ren X H. Effect of hierarchical ZSM-5 zeolite crystal size on diffusion and catalytic performance of *n*-heptane cracking. Frontiers of Chemical Science and Engineering, 2018, 12(4): 780–789
11. Sun Q M, Wang N, Xi D Y, Yang M, Yu J H. Organosilane surfactant-directed synthesis of hierarchical porous SAPO-34 catalysts with excellent MTO performance. Chemical Communications (Cambridge), 2014, 50(49): 6502–6505
12. Liu J Y, Wang J G, Li N, Zhao H, Zhou H J, Sun P C, Chen T H. Polyelectrolyte-surfactant complex as a template for the synthesis of zeolites with intracrystalline mesopores. Langmuir, 2012, 28(23): 8600–8607
13. Guo D X, Shi C X, Zhao H, Chen R, Chen S H, Sun P C, Chen T H. Polyacrylic acid as mesoscale template for synthesis of MFI zeolite with plentiful intracrystalline mesopores. Microporous and Mesoporous Materials, 2020, 293: 109821–109828
14. Shao Y C, Wang Y C, Liu X F, Li T D, Haydel P R, Tatsumi T, Wang J G. A single-crystalline hierarchical zeolite via an oriented co-growth of nanocrystals based on synergy of polyelectrolytes and hetero-atoms. ChemCatChem, 2020, 12(10): 2702–2707
15. Zhu J, Zhu Y H, Zhu L K, Rigutto M, van der Made A, Yang C G, Pan S X, Wang L, Zhu L F, Jin Y Y, et al. Highly mesoporous single-crystalline zeolite Beta synthesized using a nonsurfactant cationic polymer as a dual-function template. Journal of the American Chemical Society, 2014, 136(6): 2503–2510
16. Jin D L, Ye G H, Zheng J W, Yang W M, Zhu K, Coppens M O, Zhou X G. Hierarchical silicoaluminophosphate catalysts with enhanced hydroisomerization selectivity by directing the orientated assembly of premanufactured building blocks. ACS Catalysis, 2017, 7(9): 5887–5902
17. Schmidt I, Boisen A, Gustavsson E, Ståhl K, Pehrson S, Dahl S,

Carlsson A, Jacobsen C J H. Carbon nanotube templated growth of mesoporous zeolite single crystals. Chemistry of Materials, 2001, 13(12): 4416–4418

18. Chen H Y, Wydra J, Zhang X Y, Lee P S, Wang Z P, Fan W, Tsapatsis M. Hydrothermal synthesis of zeolites with three-dimensionally ordered mesoporous-imprinted structure. Journal of the American Chemical Society, 2011, 133(32): 12390–12393
19. Machoke A G, Beltrán A M, Inayat A, Winter B, Weissenberger T, Kruse N, Güttel R, Spiecker E, Schwieger W. Micro/Macroporous system: MFI-type zeolite crystals with embedded macropores. Advanced Materials, 2015, 27(6): 1066–1070
20. Weissenberger T, Leonhardt R, Zubiri B A, Pitínová-Štekrová M, Sheppard T L, Reiprich B, Bauer J, Dotzel R, Kahnt M, Schropp A, et al. Synthesis and characterisation of hierarchically structured titanium silicalite-1 zeolites with large intracrystalline macropores. Chemistry, 2019, 25(63): 14430–14440
21. Shi Y, Li X, Hu J K, Lu J H, Ma Y C, Zhang Y H, Tang Y. Zeolite microspheres with hierarchical structures: formation, mechanism and catalytic performance. Journal of Materials Chemistry, 2011, 21(40): 16223–16230
22. Wang P Q, Li Z B, Wang X T, Tong Y M, Yuan F L, Zhu Y J. One-pot synthesis of Cu/SAPO-34 with hierarchical pore using cupric citrate as a copper source for excellent NH_3-SCR of NO performance. ChemCatChem, 2020, 12(19): 4871–4878
23. Sun Q M, Wang N, Bai R S, Chen X X, Yu J H. Seeding induced nano-sized hierarchical SAPO-34 zeolites: cost-effective synthesis and superior MTO performance. Journal of Materials Chemistry. A, Materials for Energy and Sustainability, 2016, 4(39): 14978–14982
24. Zhang Q, Mayoral A, Terasaki O, Zhang Q, Ma B, Zhao C, Yang G J, Yu J H. Amino acid-assisted construction of single-crystalline hierarchical nanozeolites via oriented-aggregation and intraparticle ripening. Journal of the American Chemical Society, 2019, 141(9): 3772–3776
25. Ding K L, Corma A, Maciá-Agulló J A, Hu J G, Krämer S, Stair P C, Stucky G D. Constructing hierarchical porous zeolites via kinetic regulation. Journal of the American Chemical Society, 2015, 137(35): 11238–11241
26. Jacobsen C J H, Madsen C, Houzvicka J, Schmidt I, Carlsson A. Mesoporous zeolite single crystals. Journal of the American Chemical Society, 2000, 122(29): 7116–7117
27. Fang Y M, Hu H Q, Chen G H. Zeolite with tunable intracrystal mesoporosity synthesized with carbon aerogel as a secondary template. Microporous and Mesoporous Materials, 2008, 113(1–3): 481–489
28. Du J, Wang Q H, Wang Y, Guo Y N, Li R F. A hierarchical zeolite Beta with well-connected pores via using graphene oxide. Materials Letters, 2019, 250: 139–142
29. Cho H S, Ryoo R. Synthesis of ordered mesoporous MFI zeolite using CMK carbon templates. Microporous and Mesoporous Materials, 2012, 151: 107–112
30. Wei X T, Smirniotis P G. Synthesis and characterization of mesoporous ZSM-12 by using carbon particles. Microporous and Mesoporous Materials, 2006, 89(1–3): 170–178
31. Schwanke A, Villarroel-Rocha J, Sapag K, Díaz U, Corma A, Pergher S. Dandelion-like microspherical MCM-22 zeolite using BP 2000 as a hard template. ACS Omega, 2018, 3(6): 6217–6622
32. Schmidt F, Paasch S, Brunner E, Kaskel S. Carbon templated SAPO-34 with improved adsorption kinetics and catalytic performance in the MTO-reaction. Microporous and Mesoporous Materials, 2012, 164: 214–221
33. Chen H, Zhang X W, Zhang J F, Wang Q F. Controllable synthesis of hierarchical ZSM-5 for hydroconversion of vegetable oil to aviation fuel like hydrocarbons. RSC Advances, 2017, 7(73): 46109–46117
34. Varzaneh A Z, Towfighi J, Sahebdelfarb S, Bahrami H. Carbon nanotube templated synthesis of hierarchical SAPO-34 catalysts with different structure directing agents for catalytic onversion of methanol to light olefins. Journal of Analytical and Applied Pyrolysis, 2016, 121: 11–23
35. Manrique C, Guzmán A, Pérez-Pariente J, Márquez-Álvarez C, Echavarrí A. Vacuum gas-oil hydrocracking performance of Beta zeolite obtained by hydrothermal synthesis using carbon nanotubes as mesoporous template. Fuel, 2016, 182: 236–247
36. Li M R, Zhou Y P, Fang Y M. Functioned carbon nanotube templated hierarchical silicate-1 synthesis: on the existence of super-micropore. Microporous and Mesoporous Materials, 2016, 225: 392–398
37. Tao Y S, Kanoh H, Kaneko K. Uniform mesopore-donated zeolite Y using carbon aerogel templating. Journal of Physical Chemistry B, 2003, 107(40): 10974–10976
38. Tao Y S, Kanoh H, Kaneko K. ZSM-5 monolith of uniform mesoporous channels. Journal of the American Chemical Society, 2003, 125(20): 6044–6045
39. White R J, Fischer A, Goebel C, Thomas A. A sustainable template for mesoporous zeolite synthesis. Journal of the American Chemical Society, 2014, 136(7): 2715–2718
40. de la Iglesia Ó, Sánchez J L, Coronas J. Hierarchical silicalite-1 structures based on pyrolized materials. Materials Letters, 2011, 65 (19–20): 3124–3127
41. Li D, Qiu L, Wang K, Zeng Y, Li D, Williams T, Huang Y, Tsapatsis M, Wang H T. Growth of zeolite crystals with graphene oxide nanosheets. Chemical Communications, 2012, 48(16): 2249–2251
42. Ren Z, Kim E, Pattinson S W, Subrahmanyam K S, Rao C N R, Cheetham A K, Eder D. Hybridizing photoactive zeolites with graphene: a powerful strategy towards superior photocatalytic properties. Chemical Science, 2012, 3(1): 209–216
43. Zhang L C, Sun X B, Pan M, Yang X N, Liu Y C, Sun J H, Wang Q H, Zheng J J, Wang Y, Ma J H, et al. Interfacial effects between carbon nanotube templates and precursors on fabricating a wall-crystallized hierarchical pore system in zeolite crystals. Journal of Materials Science, 2020, 55(24): 10412–10426
44. Han S Y, Wang Z, Meng L Y, Jiang N Z. Synthesis of uniform mesoporous ZSM-5 using hydrophilic carbon as a hard template. Materials Chemistry and Physics, 2016, 177: 112–117
45. Bértolo R, Silva J M, Ribeiroa F, Maldonado-Hódar F J, Fernandes A, Martins A. Effects of oxidant acid treatments on carbon-templated hierarchical SAPO-11 materials: synthesis, characterization and catalytic evaluation in *n*-decane hydroisomerization. Applied Catalysis A, General, 2014, 485: 230–237
46. Zhao S F, Wang W D, Wang L Z, Schwieger W, Wang W, Huang J.

Tuning hierarchical ZSM-5 zeolite for both gas- and liquid-phase biorefining. ACS Catalysis, 2020, 10(2): 1185–1194
47. Yoo W C, Kumar S, Wang Z Y, Ergang N S, Fan W, Karanikolos G N, McCormick A V, Penn R L, Tsapatsis M, Stein A. Nanoscale reactor engineering: hydrothermal synthesis of uniform zeolite particles in massively parallel reaction chambers. Angewandte Chemie International Edition, 2008, 47(47): 9096–9099
48. Yoo W C, Kumar S, Penn R L, Tsapatsis M, Stein A. Growth patterns and shape development of zeolite nanocrystals in confined syntheses. Journal of the American Chemical Society, 2009, 131 (34): 12377–12383
49. Wang Z P, Dornath P, Chang C C, Chen H Y, Fan W. Confined synthesis of three-dimensionally ordered mesoporous imprinted zeolites with tunable morphology and Si/Al ratio. Microporous and Mesoporous Materials, 2013, 181: 8–16
50. Chen H Y, Lee P S, Zhang X Y, Lu D. Structure replication and growth development of three-dimensionally ordered mesoporous-imprinted zeolites during confined growth. Journal of Materials Research, 2013, 28(10): 1356–1364
51. Cho H J, Dornath P, Fan W. Synthesis of hierarchical Sn-MFI as Lewis acid catalysts for isomerization of cellulosic sugars. ACS Catalysis, 2014, 4(6): 2029–2037
52. Wang J, Yang M F, Shang W J, Su X P, Hao Q Q, Chen H Y, Ma X X. Synthesis, characterization, and catalytic application of hierarchical SAPO-34 zeolite with three-dimensionally ordered mesoporous imprinted structure. Microporous and Mesoporous Materials, 2017, 252: 10–16
53. Wang J, Yang M F, Zhang J B, Zhang S P, Wang X X, Fu K, Wang M Y, Sahng W J, Chen H Y, Ma X X. Fabrication of *BEA/MFI zeolite nanocomposites by confined space synthesis. Materials Chemistry and Physics, 2018, 207: 167–174
54. Madsen C, Madsen C, Jacobsen C J H. Nanosized zeolite crystals-convenient control of crystal size distribution by confined space synthesis. Chemical Communications, 1999, 8(8): 673–674
55. Schmidt I, Madsen C, Jacobsen C J H. Confined space synthesis. A novel route to nanosized zeolites. Inorganic Chemistry, 2000, 39(11): 2279–2283
56. Jacobsen C J H, Madsen C, Janssens T V W, Jakobsen H J, Skibsted J. Zeolites by confined space synthesis-characterization of the acid sites in nanosized ZSM-5 by ammonia desorption and $^{27}Al/^{29}Si$-MAS NMR spectroscopy. Microporous and Mesoporous Materials, 2000, 39(1–2): 393–401
57. Christensen C H, Johannsen K, Schmidt I, Christensen C H. Catalytic benzene alkylation over mesoporous zeolite single crystals: improving activity and selectivity with a new family of porous materials. Journal of the American Chemical Society, 2003, 125(44): 13370–13371
58. Schmidt I, Krogh A, Wienberg K, Carlsson A, Brorson M, Jacobsen C J H. Catalytic epoxidation of alkenes with hydrogen peroxide over first mesoporous titanium-containing zeolite. Chemical Communications, 2000, 21(21): 2157–2158
59. Kustova M Y, Hasselriis P, Christensen C H. Mesoporous MEL-type zeolite single crystal catalysts. Catalysis Letters, 2004, 96(3–4): 205–211
60. Kustova M Y, Rasmussen S B, Kustov A L, Christensen C H. Direct NO decomposition over conventional and mesoporous Cu-ZSM-5 and Cu-ZSM-11 catalysts: improved performance with hierarchically porous zeolites. Applied Catalysis B: Environmental, 2006, 67(1–2): 60–67
61. Xin H C, Zhao J, Xu S T, Li J P, Zhang W P, Guo X W, Hensen E J M, Yang Q H, Li C. Enhanced catalytic oxidation by hierarchically structured TS-1 zeolite. Journal of Physical Chemistry, 2010, 114(14): 6553–6559
62. Holm M S, Egeblad K, Vennestrøm P N R, Hartmann C G, Kustova M, Christensen C H. Enhancing the porosity of mesoporous carbon-templated ZSM-5 by desilication. European Journal of Inorganic Chemistry, 2008, 33(33): 5185–5189
63. Rimaz S, Halladj R, Askari S. Synthesis of hierarchal SAPO-34 nano catalyst with dry gel conversion method in the presence of carbon nanotubes as a hard template. Journal of Colloid and Interface Science, 2016, 464: 137–146
64. Deng Z Y, Zhang Y C, Zhu K, Qian G, Zhou X G. Carbon nanotubes as transient inhibitors in steam-assisted crystallization of hierarchical ZSM-5 zeolites. Materials Letters, 2015, 159: 466–469
65. Zhu K, Egeblad K, Christensen C H. Mesoporous carbon prepared from carbohydrate as hard template for hierarchically porous zeolites. European Journal of Inorganic Chemistry, 2007, 2007(25): 3955–3960
66. Song Y, Hua Z, Zhu Y, Zhou X, Wu W, Zhang L, Shi J. An *in situ* carbonaceous mesoporous template for the synthesis of hierarchical ZSM-5 zeolites by one-pot steam-assisted crystallization. Chemistry, an Asian Journal, 2012, 7(12): 2772–2776
67. Nandan D, Saxena S K, Viswanadham N. Synthesis of hierarchical ZSM-5 using glucose as a templating precursor. Journal of Materials Chemistry. A, Materials for Energy and Sustainability, 2014, 2(4): 1054–1059
68. Sun M H, Chen L H, Yu S, Li Y, Zhou X G, Hu Z Y, Sun H Y, Xu Y, Su B L. Micron-sized zeolite Beta single crystals featuring intracrystal interconnected ordered macro-meso-microporosity displaying superior catalytic performance. Angewandte Chemie International Edition, 2020, 59(44): 19582–19591
69. Sun M H, Zhou J, Hu Z Y, Chen L H, Li L Y, Wang Y D, Xie Z K, Turner S, Tendeloo G V, Hasan T, et al. Hierarchical zeolite single-crystal reactor for excellent catalytic efficiency. Mater, 2020, 3(4): 1226–1245
70. Fan W, Snyder M A, Kumar S, Lee P S, Yoo W C, Mccormick A V, Penn R L, Stein A, Tsapaysis M. Hierarchical nanofabrication of microporous crystals with ordered mesoporosity. Nature Materials, 2008, 7(12): 984–991
71. Ryoo R, Joo S H, Jun S. Synthesis of highly ordered carbon molecular sieves via template-mediated structural transformation. Journal of Physical Chemistry B, 1999, 103(37): 7743–7746
72. Jun S, Joo S H, Kruk M, Jaroniec M, Liu Z, Ohsuna T, Terasaki O. Synthesis of new, nanoporous carbon with hexagonally ordered mesostructure. Journal of the American Chemical Society, 2000, 122(43): 10712–10713
73. Zhang Y W, Okubo T, Ogura M. Synthesis of mesoporous aluminosilicate with zeolitic characteristics using vapor phase transport. Chemical Communications, 2005, 1(21): 2719–2720
74. Ogura M, Zhang Y W, Elangovan S P, Okubo T. Formation of ZMM-n: the composite materials having both natures of zeolites

and mesoporous silica materials. Microporous and Mesoporous Materials, 2007, 101(1–2): 224–230

75. Wang J, Vinu A, Coppens M O. Synthesis and structure of silicalite-1/SBA-15 composites prepared by carbon templating and crystallization. Journal of Materials Chemistry, 2007, 17(40): 4265–4273
76. Sun C, Du J M, Liu J, Yang Y, Ren N, Shen N, Xu H L, Tang Y. A facile route to synthesize endurable mesopore containing ZSM-5 catalyst for methanol to propylene reaction. Chemical Communications, 2010, 46(15): 2671–2673
77. Pei X Y, Liu X X, Liu X Y, Shan J L, Fu H, Xie Y, Yan X M, Meng X Z, Zheng Y C, Li G, et al. Synthesis of hierarchical titanium silicalite-1 using a carbon-silica-titania composite from aerogel mild carbonization. Catalysts, 2019, 9(8): 672–680
78. Xue C F, Zhang F, Wu L M, Zhao D Y. Vapor assisted "*in situ*" transformation of mesoporous carbon-silica composite for hierarchically porous zeolites. Microporous and Mesoporous Materials, 2012, 151: 495–500
79. Du J, Wang Y, Wang Y, Ma J H, Li R F. *In situ* recrystallization of mesoporous carbon-silica composite for the synthesis of hierarchically porous zeolites. Materials (Basel), 2020, 13(7): 1640–1649
80. Tanaka S, Yuan C, Miyake Y. Synthesis of silicalite-1 using an interspace of ordered mesoporous carbon-silica nanocomposites: introduction of mesoporosity in zeolite crystals. Microporous and Mesoporous Materials, 2008, 113(1–3): 418–426
81. Du J, Wang Y, Wang Y, Ma J H, Li R F. Preparation of hierarchical ZSM-5 zeolites by *in-situ* crystallization of mesoporous carbon-silica composite. ChemistrySelect, 2020, 5(44): 14130–14135
82. Kustova M, Egeblad K, Zhu K, Christensen C H. Versatile route to zeolite single crystals with controlled mesoporosity: *in situ* sugar decomposition for templating of hierarchically porous zeolites. Chemistry of Materials, 2007, 19(12): 2915–2917
83. Wang X, Li G, Wang W, Jin C, Chen Y. Synthesis, characterization and catalytic performance of hierarchical TS-1 with carbon template from sucrose carbonization. Microporous and Mesoporous Materials, 2011, 142(2–3): 494–502
84. Liu P, Jin L N, Jin C, Zhang J N, Bian S W. Synthesis of hierarchically porous silicate-1 and ZSM-5 by hydrothermal transformation of SiO_2 colloid crystal/carbon composites. Microporous and Mesoporous Materials, 2018, 262: 217–226
85. Peng Z, Chen L H, Sun M H, Zhao H, Wang Z, Li Y, Li L Y, Zhou J, Liu Z C, Su B L. A hierarchical zeolitic Murray material with a mass transfer advantage promotes catalytic efficiency improvement. Inorganic Chemistry Frontiers, 2018, 5(11): 2829–2835
86. Hou Y X, Li X Y, Sun M H, Li C F, Bakhtiar S H, Lei K, Yu S, Wang Z, Hu Z, Chen L, et al. The effect of hierarchical single-crystal ZSM-5 zeolites with different Si/Al ratios on its pore structure and catalytic performance. Frontiers of Chemical Science and Engineering, 2021, 15(2): 269–278
87. Abildstrøm J O, Ali Z N, Mentzel U V, Mielby J, Kegnæs S, Kegnæs M. Mesoporous MEL, BEA, and FAU zeolite crystals obtained by *in situ* formation of carbon template over metal nanoparticles. New Journal of Chemistry, 2016, 40(5): 4223–4227
88. Abildstrøm J O, Kegnæs M, Hytoft G, Mielby J, Kegnæs S. Synthesis of mesoporous zeolite catalysts by *in situ* formation of carbon template over nickel nanoparticles. Microporous and Mesoporous Materials, 2016, 225: 232–237
89. Wattanakit C, Warakulwit C, Pantu P, Sunpetch B, Charoenpanich M, Limtrakul J. The versatile synthesis method for hierarchical micro- and mesoporous zeolite: an embedded nanocarbon cluster approach. Canadian Journal of Chemical Engineering, 2012, 90(4): 873–880
90. Imyen T, Wannapakdee W, Limtrakul J, Wattanakit C. Role of hierarchical micro-mesoporous structure of ZSM-5 derived from an embedded nanocarbon cluster synthesis approach in isomerization of alkenes, catalytic cracking and hydrocracking of alkanes. Fuel, 2019, 254: 115593–115605
91. Tao H X, Yang H, Zhang Y H, Ren J W, Liu X H, Wang Y Q, Lu G Z. Space-confined synthesis of nanorod oriented assembled hierarchical MFI zeolite microspheres. Journal of Materials Chemistry. A, Materials for Energy and Sustainability, 2013, 1(44): 13821–13827
92. Yang H, Yang P P, Liu X H, Wang Y Q. Space-confined synthesis of zeolite Beta microspheres via steam-assisted crystallization. Chemical Engineering Journal, 2016, 299: 112–119
93. Huang Y, Ho J, Wang Z, Nakashima P, Hill A J, Wang H T. Mesoporous carbon confined conversion of silica nanoparticles into zeolite nanocrystals. Microporous and Mesoporous Materials, 2009, 117(1-2): 490–496
94. Cho S I, Choi S D, Kim J H, Kim G J. Synthesis of ZSM-5 films and monoliths with bimodal micro/mesoscopic structures. Advanced Functional Materials, 2004, 14(1): 49–54
95. Tong Y C, Zhao T B, Li F Y, Wang Y. Synthesis of monolithic zeolite Beta with hierarchical porosity using carbon as a transitional template. Chemistry of Materials, 2006, 18(18): 4218–4220
96. Martini A, Borfecchia E, Lomachenko K A, Pankin I A, Negri C, Berlier G, Beato P, Falsig H, Bordiga S, Lamberti C. Composition-driven Cu-speciation and reducibility in Cu-CHA zeolite catalysts: a multivariate XAS/FTIR approach to complexity. Chemical Science (Cambridge), 2017, 8(10): 6836–6851
97. Zhao Z C, Yu R, Zhao R R, Shi C, Gies H, Xiao F S, De Vos D, Yokoi T, Bao X H, Kolb U, et al. Cu-exchanged Al-rich SSZ-13 zeolite from organotemplate-free synthesis as NH_3-SCR catalyst: effects of Na^+ ions on the activity and hydrothermal stability. Applied Catalysis B: Environmental, 2017, 217: 421–428
98. Zhu P F, Yang G H, Sun J, Fan R, Zhang P P, Yoneyama Y, Tsubaki N. A hollow Mo/HZSM-5 zeolite capsule catalyst: preparation and enhanced catalytic properties in methane dehydroaromatization. Journal of Materials Chemistry. A, Materials for Energy and Sustainability, 2017, 5(18): 8599–8607
99. Gu J, Zhang Z Y, Ding L P, Huang K, Xue N H, Peng L M, Guo X F, Ding W P. Platinum nanoparticles encapsulated in HZSM-5 crystals as an efficient catalyst for green production of *p*-aminophenol. Catalysis Communications, 2017, 97: 98–101
100. Choi M, Wu Z J, Iglesia E. Mercaptosilane-assisted synthesis of metal clusters within zeolites and catalytic consequences of encapsulation. Journal of the American Chemical Society, 2010, 132(26): 9129–9137
101. Wang N, Sun Q M, Bai R S, Li X, Guo G Q, Yu J H. *In situ* confinement of ultrasmall Pd clusters within nanosized silicalite-1 zeolite for highly efficient catalysis of hydrogen generation.

Journal of the American Chemical Society, 2016, 138(24): 7484–7487

102. Sánchez-Sánchez M, Manjón Sanz A, Díaz I, Mayoral Á, Sastre E. Micron-sized single-crystal-like CoAPO-5/carbon composites leading to hierarchical CoAPO-5 with both inter-and intracrystalline mesoporosity. Crystal Growth & Design, 2013, 13(6): 2476–2485
103. Varzaneh A Z, Towfighi J, Sahebdelfar S. Carbon nanotube templated synthesis of metal containing hierarchical SAPO-34 catalysts: impact of the preparation method and metal avidities in the MTO reaction. Microporous and Mesoporous Materials, 2016, 236: 1–12
104. Flores C, Batalha N, Ordomsky V V, Zholobenko V L, Baaziz W, Marcilio N R, Khodakov A Y. Direct production of iso-paraffins from syngas over hierarchical cobalt-ZSM-5 nanocomposites synthetized by using carbon nanotubes as sacrificial templates. ChemCatChem, 2018, 10(10): 2291–2299
105. Flores C, Zholobenko V L, Gu B, Batalha N, Valtchev V, Baaziz W, Ersen O, Marcilio N R, Ordomsky V V, Khodakov A Y. Versatile roles of metal species in carbon nanotube templates for the synthesis of metal-zeolite nanocomposite catalysts. ACS Applied Nano Materials, 2019, 2(7): 4507–4517
106. Amoo C C, Li M, Noreen A, Fu Y, Maturura E, Du C, Yang R, Gao X, Xing C, Tsubaki N. Fabricating Fe nanoparticles embedded in zeolite Y microcrystals as active catalysts for Fischer-Tropsch synthesis. ACS Applied Nano Materials, 2020, 3(8): 8096–8103
107. Chen Y Y, Chang C J, Lee H V, Juan J C, Lin Y C. Gallium-immobilized carbon nanotubes as solid templates for the synthesis of hierarchical Ga/ZSM-5 in methanol aromatization. Industrial & Engineering Chemistry Research, 2019, 58(19): 7948–7956
108. Chang C J, Chen C H, Lee J F, Sooknoi T, Lin Y C. Ga-supported MFI zeolites synthesized using carbon nanotubes containing gallium oxide nanoparticles on exterior walls and in interior channels as hard templates for methanol aromatization. Industrial & Engineering Chemistry Research, 2020, 59(24): 11177–11186